Range Extension Control System for Electric Vehicles Based on Optimal-Deceleration Trajectory and Front-Rear Driving-Braking Force Distribution Considering Maximization of Energy Regeneration

Shingo Harada and Hiroshi Fujimoto
The University of Tokyo
5-1-5, Kashiwanoha, Kashiwa, Chiba, 277-8561 Japan
Phone: +81-4-7136-3881
Fax: +81-4-7136-3881
Email: harada@hflab.k.u-tokyo.ac.jp, fujimoto@k.u-tokyo.ac.jp

***Abstract*— Electric vehicles (EVs) have become a world-widely recognized solution for future green transportation. However, the mileage per charge of EVs is short compared with that of internal combustion engine vehicles. In this paper, a maximization method of regenerative energy is proposed. The method optimizes the velocity trajectory and distribution ratio of front and rear braking force using calculus of variations. The effectiveness of the proposed method is verified by simulations and experiments.**

I. Introduction

Considering current environmental and energy problems, electric vehicles (EVs) have been proposed as an alternative solution to internal combustion engine vehicles (ICEVs). In addition, EVs have the remarkable advantages compared with ICEVs [1].

- Response of driving-braking force by motor is much faster than that of engines (100 times).
- In-wheel motors enable independent control and drive of each wheel.
- Motor torque is measured precisely from motor current.

Research of traction control [2], [3] and stability control [4] utilizing the above advantages were actively conducted.

One of the reasons that prevents EVs from spreading is that mileage per charge of EVs is shorter than that of conventional ICEVs. In order to solve this problem, research on efficiency improvement of motors [5] and extending high efficiency area of motor [6] were carried out. From the view point of motor efficiency control, research of torque and angular velocity pattern that maximize efficiency during acceleration and deceleration [7] was carried out. Utilizing independent characteristic of traction motors, a torque distribution method was studied to decrease EV's energy consumption [8].

On the other hand, the authors' research group proposed range extension control systems (RECSs) [9]–[11]. These systems do not involve changes of vehicle structure such as additional clutch [8] and motor type. RECS extends cruising range by motion control of vehicle.

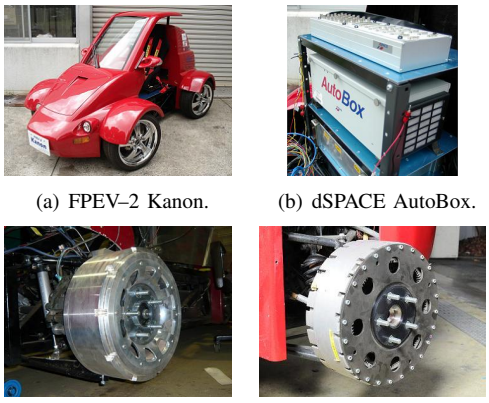

(a) FPEV–2 Kanon. (b) dSPACE AutoBox.

(c) Front motor. (d) Rear motor.

Fig. 1. Experimental vehicle.

Conventional research in RECS has been conducted under an assumption that vehicle motion is controlled by driver. However, it is needed to consider autonomous driving technologies along with the development of intelligent transport systems (ITS) [12]. If vehicle velocity can be controlled, minimizing the energy consumption by optimizing the velocity trajectory is possible.

In this paper, for electric vehicles which are equipped with front and rear motors, a RECS which maximizes the regenerative energy is proposed. This method optimizes the velocity trajectory and braking force distribution ratio. The proposed method can be applied to acceleration. The effectiveness of the proposed method is verified by simulations and experiments.

II. Experimental Vehicle and Vehicle Model

A. Experimental Vehicle

In this research, an original electric vehicle "FPEV–2 Kanon", manufactured by the authors' research group, is used. This vehicle has four outer-rotor type in-wheel motors. Since these motors are direct drive type, the reaction force from road is directly transferred to the motor without backlash influence of the reduction gear.

TABLE I

VEHICLE SPECIFICATION.

Vehicle Mass M	854 kg
Wheelbase l	1.715 m
Distance from CG to front/rear axle l_f, l_r	l_f:1.013 m l_r:0.702 m
Gravity height h_g	0.51 m
Front Wheel Inertia J_{ω_f}	1.24 Nms^2
Rear Wheel Inertia J_{ω_r}	1.26 Nms^2
Wheel Radius r	0.302 m

TABLE II

SPECIFICATION OF IN–WHEEL MOTORS.

	Front	Rear
Manufacturer	TOYO DENKI SEIZO K.K.	
Type	Direct Drive System Outer Rotor Type	
Rated Torque	110 Nm	137 Nm
Maximum Torque	500 Nm	340 Nm
Rated Power	6.0 kW	4.3 kW
Maximum Power	20.0 kW	10.7 kW
Rated Speed	382 rpm	300 rpm
Maximum Speed	1113 rpm	1500 rpm

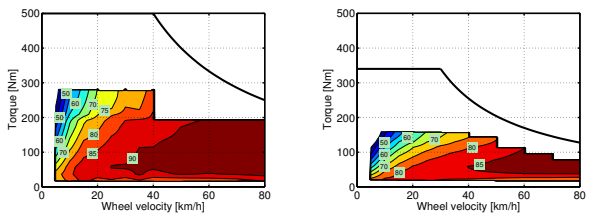

(a) Front motor. (b) Rear motor.

Fig. 2. Efficiency maps of front and rear motors.

Fig. 1 shows the experimental vehicle. The dSPACE AutoBox (DS1103) is used for real-time data acquisition and control. Table I and Table II show the specification of vehicle and in-wheel motors. Fig. 2 expresses efficiency map of the front/rear in-wheel motors. Since front/rear motors installed in the vehicle are different, efficiency maps of those are different. Therefore, extending cruising range by exploiting the difference of the efficiency is possible.

Fig. 3 illustrates power system of the vehicle. Lithium-ion battery is used as power source. The voltage of the main battery is 160 V (ten battery modules are connected in series). The voltage is boosted to 320 V by a chopper. In this paper, the chopper loss is neglected.

B. Vehicle Model

In this section, a four wheel driven vehicle model is described. The equation of wheel rotation is expressed by (1), as shown in Fig. 4. In case of straight driving, driving-braking forces of right and left wheels are equal. From Fig. 5, the equations of vehicle dynamics are expressed as (2) and (3)

$$J_{\omega_j}\dot{\omega}_j = T_j - rF_j, \tag{1}$$

$$M\dot{V} = F_{\mathrm{all}} - F_{\mathrm{DR}}, \tag{2}$$

$$F_{\mathrm{all}} = 2(F_f + F_r), \tag{3}$$

where ω_j[rad/s] is the wheel angular velocity, V[m/s] is the vehicle velocity, T_j[Nm] is the motor torque, F_{all}[N] is the total driving-braking force, F_j[N] is the driving-braking force of each wheel, M[kg] is the vehicle mass, r[m] is the wheel radius, J_{ω_j}[Nms^2] is the wheel inertia, and F_{DR}[N] is the driving resistance. The subscript j represents f or r (f stands for front and r represents rear).

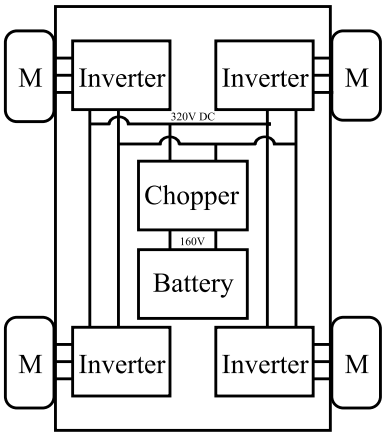

Fig. 3. Electric power system of vehicle.

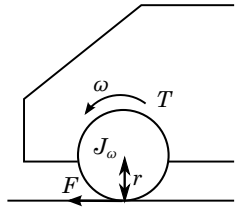

Fig. 4. Rotational motion of wheel.

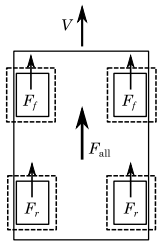

Fig. 5. Vehicle model.

C. Driving-Braking force distribution model

During straight driving, required total driving-braking force can be distributed to each wheel. In this research, since the motors of the EV can be independently controlled, a degree of freedom of the driving-braking force distribution exists. Introducing front and rear driving-braking force distribution ratio k, driving-braking forces can be formulated based on the total driving-braking force F_{all} and the distribution ratio k, as follows [10]:

$$F_f = \frac{1}{2}(1-k)F_{\mathrm{all}}, \tag{4}$$

$$F_r = \frac{1}{2}kF_{\mathrm{all}}. \tag{5}$$

Distribution ratio k varies from 0 to 1. $k = 0$ means the vehicle is a front driven system, and $k = 1$ means rear driven only.

III. OPTIMAL VELOCITY TRAJECTORY AND DISTRIBUTION RATIO

A. Constant Deceleration (Trajectory 1)

In this paper, a case that a vehicle which has velocity V_0 at t_0 starts to decelerate and stop at t_1 is considered.

As the first trajectory, constant deceleration is employed. In this case, velocity trajectory and braking time t_1 are given by

$$V_1(t) = V_0 - \frac{V_0^2}{2X}t \quad (t_0 \le t \le t_1), \tag{6}$$

$$t_1 = \frac{2X}{V_0}, \tag{7}$$

where V_0[m/s] is initial velocity, X[m] is braking distance.

B. Modeling of Regenerative Energy

To derive optimal deceleration trajectory and braking force distribution ratio, regenerative energy is expressed. Neglecting the inverter loss, iron and mechanical loss of the motors, the sum of input power of each inverter $P_{\rm in}$ is expressed as

$$P_{\rm in} = P_{\rm out} + P_c, \tag{8}$$

where $P_{\rm out}$[W] is the sum of mechanical output of each motor, P_c[W] is the sum of copper loss of each motor. In this paper, the slip ratio of each wheel is neglected. Therefore, ω_j is expressed as $\omega_j = V/r$. Then, from (1) and (2), $P_{\rm out}$ is given by

$$\begin{aligned} P_{\rm out} &= 2(\omega_f T_f + \omega_r T_r) \\ &= \left\{ M + \frac{2}{r^2}(J_{\omega_f} + J_{\omega_r}) \right\} \dot{V}V + F_{\rm DR}(V)V. \end{aligned} \tag{9}$$

In the modeling of copper loss P_c, let us suppose that magnet torque is much bigger than reluctance torque, and q-axis current is much bigger than d-axis current. In this case, P_c is expressed as

$$P_c = 2(R_f i_{qf}^2 + R_r i_{qr}^2), \tag{10}$$

where $R_j[\Omega]$ is the armature winding resistance of the motor, i_{qj}[A] is q-axis current of the motor. Then, following relationship between q-axis current and torque is obtained,

$$i_{qj} = \frac{T_j}{K_{tj}}, \tag{11}$$

where K_{tj}[Nm/A] is the torque coefficient of the motor. Therefore, from (1), (2), (4) and (5), copper loss P_c is given by

$$\begin{aligned} P_c &= 2(R_f i_{qf}^2 + R_r i_{qr}^2) \\ &= 2\left(\frac{R_f T_f^2}{K_{tf}^2} + \frac{R_r T_r^2}{K_{tr}^2} \right) \\ &= 2\left[\frac{R_f}{K_{tf}^2} \left\{ \frac{J_{\omega_f}}{r}\dot{V} + \frac{r}{2}(1-k)\left(M\dot{V} + F_{\rm DR}(V) \right) \right\}^2 \right. \\ &\quad \left. + \frac{R_r}{K_{tr}^2} \left\{ \frac{J_{\omega_r}}{r}\dot{V} + \frac{r}{2}k\left(M\dot{V} + F_{\rm DR}(V) \right) \right\}^2 \right], \end{aligned} \tag{12}$$

In addition, driving resistance $F_{\rm DR}$[N] is determined as

$$F_{\rm DR}(V) = \mu_0 Mg + f_{\rm DR}(V), \tag{13}$$

where μ_0 is rolling friction coefficient, $f_{\rm DR}(V)$ is assumed to be propotional to V. The coefficient of $f_{\rm DR}(V)$ is determined as b.

From (9), (12) and (13), $P_{\rm in}$ is described as

$$\begin{aligned} &P_{\rm in}(k, V, \dot{V}) \\ &\quad = a_{20}(k)\dot{V}^2 + a_{11}(k)\dot{V}V + a_{10}(k)\dot{V} \\ &\qquad + a_2(k)V^2 + a_1(k)V + a_0(k), \end{aligned} \tag{14}$$

where

$$\begin{cases} a_{20}(k) &= \frac{2R_f}{K_{tf}^2}\left\{ \frac{J_{\omega_f}}{r} + \frac{Mr}{2}(1-k) \right\}^2 \\ & \quad + \frac{2R_r}{K_{tr}^2}\left(\frac{J_{\omega_r}}{r} + \frac{Mr}{2}k \right)^2, \\ a_{11}(k) &= M + \frac{2}{r^2}(J_{\omega_f} + J_{\omega_r}) \\ & \quad + \frac{2bR_r}{K_{tr}^2}\left(J_{\omega_r} + \frac{Mr^2}{2}k \right)k \\ & \quad + \frac{2bR_f}{K_{tf}^2}\left\{ J_{\omega_f} + \frac{Mr^2}{2}(1-k) \right\}(1-k), \\ a_{10}(k) &= \frac{2\mu_0 MgR_r}{K_{tr}^2}\left(J_{\omega_r} + \frac{Mr^2}{2}k \right)k \\ & \quad + \frac{2\mu_0 MgR_f}{K_{tf}^2}\left\{ J_{\omega_f} + \frac{Mr^2}{2}(1-k) \right\}(1-k), \\ a_2(k) &= b + \frac{b^2r^2}{4}\left\{ \frac{R_f}{K_{tf}^2}(1-k)^2 + \frac{R_r}{K_{tr}^2}k^2 \right\}, \\ a_1(k) &= \mu_0 Mg \\ & \quad + \frac{\mu_0^2 M^2 g^2 b r^2}{2}\left\{ \frac{R_f}{K_{tf}^2}(1-k)^2 + \frac{R_r}{K_{tr}^2}k^2 \right\}, \\ a_0(k) &= \frac{\mu_0^2 M^2 g^2 r^2}{2}\left\{ \frac{R_f}{K_{tf}^2}(1-k)^2 + \frac{R_r}{K_{tr}^2}k^2 \right\}. \end{cases}$$

By using $P_{\rm in}$, regenerative energy W[Ws] is given as

$$W = -\int_{t_0}^{t_1} P_{\rm in}(k, V, \dot{V})dt. \tag{15}$$

The objective of this paper is to maximize $W_{\rm in}$ by optimizing k and V.

C. Derivation of Optimal Deceleration Trajectory and Driving Force Distribution Ratio

1) Case with given braking distance and time (Trajectory 2): In the case braking distance is known, a condition about vehicle velocity is given by

$$\int_{t_0}^{t_1} V(t)dt = X. \tag{16}$$

In this section, a variational problem is solved to derive the trajectory of V which satisfies (16) and maximizes regenerative energy written by (15). The solution of variational problem which contains such incidental condition is given by solving the simultaneous equations which have Lagrange multiplier λ [13] such as

$$\frac{\partial P_{\rm in}(k, V, \dot{V})}{\partial k} = 0, \tag{17}$$

$$\begin{aligned} &\frac{d}{dt}\left(\frac{\partial P_{\rm in}(t, k, V, \dot{V})}{\partial \dot{V}} \right) - \frac{\partial P_{\rm in}(t, k, V, \dot{V})}{\partial V} \\ &+\lambda\left\{ \frac{d}{dt}\left(\frac{\partial V}{\partial \dot{V}} \right) - \frac{\partial V}{\partial V} \right\} = 0. \end{aligned} \tag{18}$$

In (8) and (17), by assuming the inertia of wheels to be much smaller than vehicle mass, the optimal driving force

distribution ratio k_{opt} expressed by (19) is obtained.

$$k_{\mathrm{opt}} = \frac{\frac{R_f}{K_{tf}^2}}{\frac{R_f}{K_{tf}^2} + \frac{R_r}{K_{tr}^2}} \tag{19}$$

k_{opt} is the distribution ratio which minimizes the copper loss. k_{opt} consists of only motor parameters, therefore k_{opt} is constant. In addition, from (14) and (18), the below equation is given.

$$2a_{20}(k)\ddot{V} - 2a_2(k)V = a_1(k) + \lambda \tag{20}$$

In case of k is constant, (20) can be solved analytically. Therefore, the optimal velocity trajectory with given braking distance and time is obtained as

$$V_2(t,k) = A_1 e^{\alpha(k)t} + B_1 e^{-\alpha(k)t} + \beta_1(k), \tag{21}$$

where

$$\alpha(k) = \sqrt{\frac{a_2(k)}{a_{20}(k)}} \tag{22}$$

$$\beta_1(k) = -\frac{a_1(k) + \lambda}{2a_2(k)}$$

The integration constants A_1, B_1 and λ are calculated to satisfy $V_2(t_0,k) = V_0, V_2(t_1,k) = 0$ and (16) after deciding k.

2) Case with given braking time (Trajectory 3): In the case with given braking time, the optimal velocity trajectory is obtained by solving the differential equation with $\lambda = 0$ in (20).

$$2a_{20}(k)\ddot{V} - 2a_2(k)V = a_1(k) \tag{23}$$

Similarly, solving the differential equation, the optimal velocity trajectory with only braking time is expressed as

$$V_3(t,k) = A_2 e^{\alpha(k)t} + B_2 e^{-\alpha(k)t} + \beta_2(k), \tag{24}$$

where

$$\beta_2(k) = -\frac{a_1(k)}{2a_2(k)}. \tag{25}$$

The integration constants A_2 and B_2 are also calculated to satisfy $V_3(t_0,k) = V_0, V_3(t_1,k) = 0$ after deciding k.

IV. Simulation

In this section, to demonstrate the effectiveness of the proposed method, simulation is conducted. To represent the relationship between road and tire, Magic Formula [14] is used. μ_0 and b which is the coefficient of $f_{DR}(V)$ are set as 8.36×10^{-3} and 10.7 Ns/m, respectively. These values are obtained by experiments. The initial condition is determined to $V_0 = 30$ km/h, $t_0 = 0$ s. In this paper, 6 cases are considered. The distribution ratio is $k = 0.5, k_{\mathrm{opt}}$. Three types of trajectories are calculated under each distribution ratio. To compare all cases under same braking distance, braking time of each case is decided as Table III. In this paper, case (A) is treated as conventional method. Case (E) and (F) are proposed method 1 and 2, respectively. The braking distance is set to 27.38 m.

TABLE III

Braking time [s](V_0 = 30 km/h, X = 27.38 m).

k	Trajectory 1	Trajectory 2	Trajectory 3
0.5	6.57 (A) (Conventional)	6.57 (B)	7.87 (C)
k_{opt}	6.57 (D)	6.57 (E) (Proposed 1)	10.0 (F) (Proposed 2)

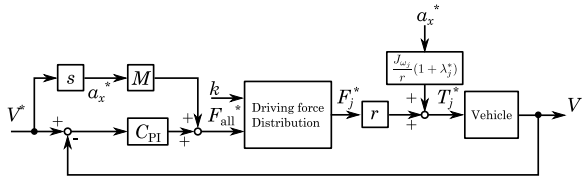

Fig. 6. Vehicle speed control system.

In this paper, automatic control of vehicle velocity is assumed to be possible as described in section 1. Fig. 6 shows vehicle velocity control system to control the vehicle automatically. This system is composed of a feedforward controller and feedback controller. The input is vehicle velocity reference V^*, and these controllers generate total driving-braking force reference F_{all}^*. And then, F_{all}^* is distributed to the front and rear driving-braking force reference F_j^* based on (4) and (5). Represented by the slip ratio, front and rear torque reference T_j^* is given as

$$T_j^* = rF_j^* + \frac{J_{\omega_j} a_x^*}{r}(1 + \lambda_j^*), \tag{26}$$

where the second term of right hand side means compensation of inertia of the wheels. In this research, considering stability of vehicle velocity control system, reference of the acceleration a_x^* is used. λ_j^* is nominal slip ratio of front and rear wheels that is 0.05, 0 and -0.05 during acceleration, cruising and deceleration, respectively.

Vehicle velocity controller $C_{\mathrm{PI}}(s)$ is a PI controller, and it is designed by pole placement method. The plant of vehicle velocity controller is expressed as

$$\frac{V}{F_{\mathrm{all}}} = \frac{1}{Ms}. \tag{27}$$

In the simulation and experiment, the pole of vehicle velocity controller is set to -5 rad/s.

Fig. 7 shows simulation results. Fig. 7(a), Fig. 7(b) and Fig. 7(c) show vehicle velocity of case (A), (E) and (F), respectively. From these figures, case (E) and (A) are almost equivalent. On the other hand, in case (F), the initial deceleration is large. Therefore, as shown Fig. 7(d) and Fig. 7(e), the braking force at start in case (F) is larger than that of case (A). From a standpoint of velocity trajectory, the difference between case (E) and (A) is slight. However front and rear braking force of each case is different because of the different distribution ratio. Fig. 7(f) shows inverter input power. In case (F), the regenerative energy is larger than that of other cases

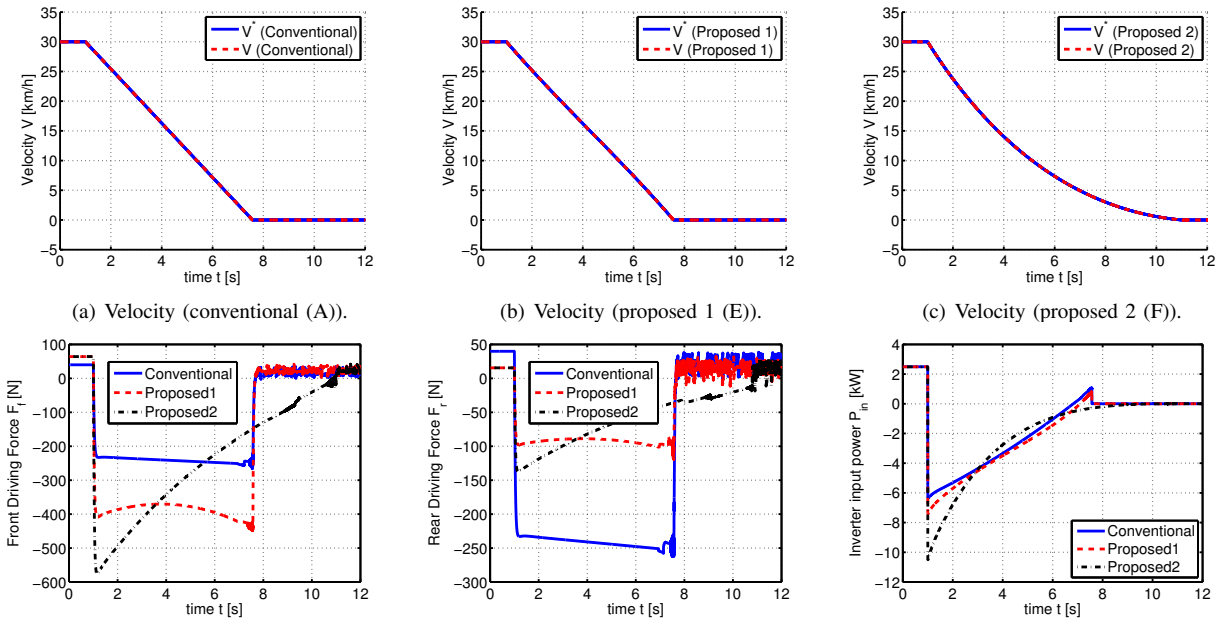

(a) Velocity (conventional (A)). (b) Velocity (proposed 1 (E)). (c) Velocity (proposed 2 (F)).

(d) Front driving force. (e) Rear driving force. (f) Inverter input power.

Fig. 7. Simulation result (conventional (A), proposed 1 (E), proposed 2 (F)).

TABLE IV
REGENERATIVE ENERGY [KWS] (SIMULATION RESULT).

k	Trajectory 1	Trajectory 2	Trajectory 3
0.5	18.99 (A) (Conventional)	19.01 (B)	19.96 (C)
k_{opt}	21.18 (D)	21.20 (E) (Proposed 1)	22.08 (F) (Proposed 2)

immediately after starting brake. In addition, in case (F), the vehicle does not consume the energy just before stop, although the case (A) and (E) consume energy.

Table IV shows the regenerative energy in the simulation. From comparisons between (A) and (B) and between (D) and (E), the effectiveness of optimization of trajectory under the same braking time and distance as conventional method is slight. However, from comparisons between (A) and (C) and between (D) and (F), the regenerative energy of optimal trajectory with the same braking distance improved about 4 or 5 %. On the other hand, the effectiveness of changing k from 0.5 to k_{opt} is great. The regenerative energy improved about 10 %, respectively. As a result, proposed method 1 (E) and 2 (F) improved about 12 % and 16 % compared with conventional method (A), respectively.

V. EXPERIMENT

Experiments are conducted under the same condition as simulation. In the experiments, the average of all the wheel velocities is treated as vehicle velocity V. Inverter input power P_{in} is calculated as

$$P_{\mathrm{in}} = V_{\mathrm{dc}}(I_{\mathrm{dc}f} + I_{\mathrm{dc}r}), \tag{28}$$

where V_{dc}[V] is the inverter input voltage, $I_{\mathrm{dc}f}$[A] is the front inverter input current, and $I_{\mathrm{dc}r}$[A] is rear inverter input current. P_{in} includes inverter loss and motor iron loss.

Fig. 8 shows experimental results. From Fig. 8(d) and Fig. 8(e), the absolute value of front and rear braking force differ from simulation results because of modeling error of driving resistance. Although, from Fig. 8(f), the results of inverter input power show the same tendency as simulation results.

Table V shows the regenerative energy in the experiments. The average values and standard deviations of 7 times experiments are shown. Similar to simulation, the effectiveness of velocity trajectory optimization with the same braking time and distance as proposed method is slight. On the other hand, the regenerative energy improved about 4 % with only the same braking distance, and improved about 11 % due to optimization of velocity trajectory and distribution ratio. As a result, proposed method 1 (E) and 2 (F) improved about 11 % and 16 % compared with conventional method (A), respectively.

VI. CONCLUSION

In this paper, as a range extension control system for acceleration process, an optimization method of vehicle velocity trajectory and front and rear driving-braking force distribution ratio is proposed. The proposed optimization method was applied to two deceleration trajectories: 1) given braking distance and time and 2) given braking time. In the experimental results, proposed method 1 and 2 increase regenerative energy about 11 % and 16 %, respectively.

The future work is to introduce load transfer, slip ratio and motor iron loss into the loss model.

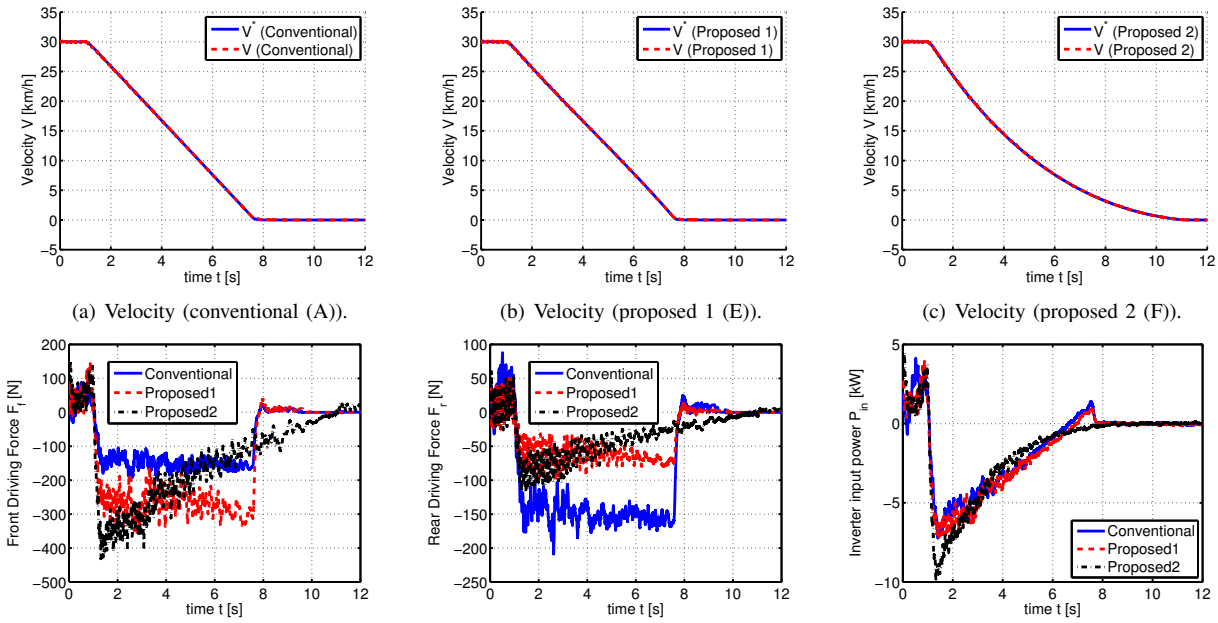

(a) Velocity (conventional (A)).

(b) Velocity (proposed 1 (E)).

(c) Velocity (proposed 2 (F)).

(d) Front driving force.

(e) Rear driving force.

(f) Inverter input power.

Fig. 8. Experimental result (conventional (A), proposed 1 (E), proposed 2 (F)).

TABLE V

REGENERATIVE ENERGY [kWs] (EXPERIMENTAL RESULT: AVERAGE±STANDARD DEVIATION).

k	Trajectory 1	Trajectory 2	Trajectory 3
0.5	17.94±0.14 (A) (Conventional)	17.96±0.08 (B)	18.73±0.14 (C)
k_{opt}	19.95±0.24 (D)	19.97±0.19 (E) (Proposed 1)	20.80±0.25 (F) (Proposed 2)

ACKNOWLEDGEMENT

This research was partly supported by Industrial Technology Research Grant Program from New Energy and Industrial Technology Development Organization(NEDO) of Japan (number 05A48701d), and by the Ministry of Education, Culture, Sports, Science and Technology grant (number 22246057).

REFERENCES

[1] Y. Hori: "Future Vehicle Driven by Electricity and Control–Research on Four–Wheel–Motored:"UOT Electric March II"", IEEE Trans. IE, Vol. 51, No. 5, pp. 954–962 (2004)

[2] R. Shirato, T. Akiba, T. Fujita and S. Shimodaira: "A Study of Novel Traction Control Method for Electric Propulsuon Vehicle", Journal of the Society of Instrument and Control Engineers, Vol. 50, No. 3, pp. 195–200 (2011) (in Japanese)

[3] K. Maeda, H. Fujimoto, Y. Hori: "Four–wheel Driving–force Distribution Method Based on Driving Stiffness and Slip Ratio Estimation for Electric Vehicle with In–wheel Motors", the 8th IEEE Vehicle Power and Propulsion Conference, pp. 1286–1291 (2012)

[4] N. Ando, H. Fujimoto: "Yaw–rate control for electric vehicle with active front/rear steering and driving/braking force distribution of rear wheels", in Proc. the 11th IEEE International Workshop on Advanced Motion Control, pp. 726–731 (2010)

[5] H. Toda, Y. Oda, M. Kohno, M. Ishida, and Y. Zaizen: "A New High Flux Density Non–Oriented Electrical Steel Sheet and its Motor Performance", IEEE Trans. MAGNETICS, Vol. 48, No. 11, pp. 3060–3063 (2012)

[6] H. Hijikata, T. Shigeta, N. Kariya, K. Akatsu, and T. Kato: "A Study of Dual Winding Method for Compound Magnetomotive Force Motor", IEEJ Trans. IA, Vol. 133, No. 10, pp. 986–994 (2013) (in Japanese)

[7] K. Inoue, K. Kotera, Y. Asano, and T. Kato: "Optimal Torque and Rotating Speed Trajectories Minimizing Energy Loss of Induction Motor Under Both Torque and Speed Limits", in Proc. Power Electronics and Drive Systems, 2013 IEEE 10th International Conference, pp. 1127–1132 (2013)

[8] X. Yuan and J. Wang: "Torque Distribution Strategy for a Front– and Rear–Wheel–Driven Electric Vehicle", IEEE Trans. Veh. Technol., Vol. 61, No. 8, pp. 3365–3374 (2012)

[9] H. Fujimoto and H. Sumiya: "Range Extension Control System of Electric Vehicle Based on Optimal Torque Distribution and Cornering Resistance Minimization", in Proc. 37th Annual Conference of the IEEE Industrial Electronics Society, pp. 3727–3732 (2011)

[10] H. Fujimoto, S. Egami, J. Saito, and K. Handa: "Range Extension Control System for Electric Vehicle Based on Searching Algorithm of Optimal Front and Rear Driving Force Distribution", in Proc. 38th Annual Conference of the IEEE Industrial Electronics Society, pp. 4244–4249 (2012)

[11] S. Harada, H. Fujimoto: "Range Extension Control System for Electric Vehicles during Acceleration and Deceleration Based on Front and Rear Driving-Braking Force Distribution Considering Slip Ratio and Motor Loss", in Proc. 39th Annual Conference of the IEEE Industrial Electronics Society, pp. 6624–6629 (2013)

[12] S. E. Shladover: "Cooperative (rather than autonomous) Vehicle-Highway Automation Systems", Intelligent Transportation Systems Magazine, IEEE, Vol. 1, No. 1, pp. 10–19 (2009)

[13] I. M. Gelfand and S. V. Fomin: "Calculus of Variations", trans. R. A. Silverman, DOVER PUBLICATIONS, INC. (2000)

[14] H. B. Pacejka and E. Bakker: "The Magic Formula Tyre Model", Vehicle System Dynamics: International Journal of Vehicle Mechanics and Mobility, Vol. 21, No. 1, pp. 1–18 (1992)